FIREBALL : The first ultraviolet fiber fed spectrograph

Sarah E. Tuttle[a], David Schiminovich[a], Robert Grange[c], Shahin Rahman[b], Mateusz Matuszewski[b], Bruno Milliard[c], Jean-Michel Deharveng[c] and D. Christopher Martin[b]

[a]Columbia University Astronomy Department, 550 W. 120th St., New York, NY 10027, USA;
[b]Caltech, Cahill Center for Astrophysics, 1216 E California Blvd., Pasadena, CA 91125, USA;
[c]Laboratoire d'Astrophysique de Marseille, 13388 Marseille CEDEX 13, France

ABSTRACT

FIREBall (the Faint Intergalactic Redshifted Emission Balloon) is a balloon-borne 1m telescope coupled to an ultraviolet fiber-fed spectrograph. FIREBall is designed to study the faint and diffuse emission of the warm hot intergalactic medium, until now detected primarily in absorption. FIREBall is a pathfinding mission to test new technology and make new constraints on the temperature and density of this gas. FIREBall has flown twice, the most recent flight (June 2009) a fully functioning science flight. Here we describe the spectrograph design, current setup, and calibration measurements from the campaign.

Keywords: Cosmology, Integral Field Spectroscopy, FIREBALL, UV Spectroscopy, Fiber spectrograph, IGM, CGM

1. INTRODUCTION

The FIREBall spectrograph is the first UV fiber-fed integral field unit to be built and used. It is a central component of the FIREBall experiment. Below I detail the spectrograph's optical and mechanical design, assembly, and testing before flight. The FIREBall spectrograph has been flown twice, and small differences in the flight configurations will be noted throughout. A summary of changes is found in Section 4.

The spectrograph mounts below the siderostat on the gondola floor. The spectrograph design incorporates an all-reflective folded-Offner style design enclosed in an aluminum vacuum housing. A fiber optic bundle IFU feeds light from the focal plane of the telescope to the spectrograph. The spectrograph IFU contains 281 close-packed and ordered fibers, with a field of view of 2.3 arcminutes in diameter. The fibers are 100 μm diameter core, each 8" on the sky in diameter. The spectrograph parameters are summarized in table 1 and are discussed in this section in more detail.

2. OPTICAL AND MECHANICAL DESIGN

A requirement of the FIREBall spectrograph is that it needs to be compact and efficient, with limited aberrations across a wide detector area. The structure must be mechanically robust and stable for the changeable environment encountered during balloon flight. The balloon platform and telescope design place limits on the mass and footprint of the spectrograph which are met by a simple optical layout. The balloon atmospheric window limits observations to a narrow bandpass ($\lambda_0 \sim 210$nm, $\Delta\lambda < 30$nm). This makes an all reflective design feasible, as the throughput can be optimized for the bandpass. Requiring high reflectance over a wider bandpass would make the optical coating design more difficult.

2.1 Optical Design

The design can be best described as a "folded" Offner spectrograph. The Offner spectrograph is an Offner relay modified to a spectrograph through the replacement of a convex mirror with a convex grating used in the order -1 in a near Littrow condition. This style of spectrograph shares some design features with the earlier Czerny-Turner spectrographs, but with decreased distortion and improved image quality. The fold allows for a compact

Further author information:
S.E.T.: sarah@astro.columbia.edu

Space Telescopes and Instrumentation 2010: Ultraviolet to Gamma Ray,
edited by Monique Arnaud, Stephen S. Murray, Tadayuki Takahashi, Proc. of SPIE Vol. 7732,
773227 · © 2010 SPIE · CCC code: 0277-786X/10/$18 · doi: 10.1117/12.857877

Table 1. Spectrograph Parameters

Parameter	Value (Flight 2)
Spectrograph F/#	2.5
Spectrograph Resolution (R)	5000
Grating Groove Density (2nd flight)	5000 g/mm (4800 g/mm)
Fiber Numerical Aperture	0.22
Plate Scale	12 μ m
Angular Resolution	10 arcseconds (FWHM)
Field of View (fiber)	8.3 arcseconds
Field of View (total)	140x140 arcseconds^2
Science Fibers	342 (281)
Calibration Fibers	19 (37)
Thermal Shielding	MLI (None)
Focus Stage	No (Flight-ready)
Spectrograph Interior	Aluminum (Painted Black)

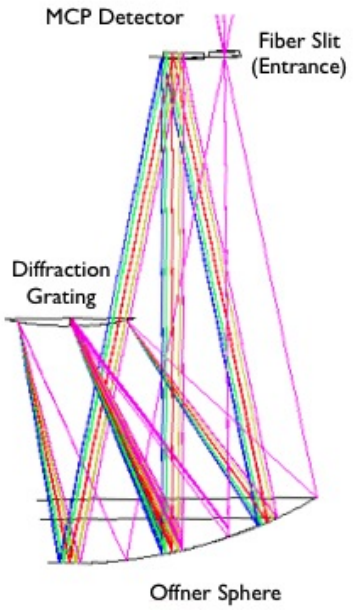

Figure 1. The Zemax raytrace for the FIREBall spectrograph. The pupil fan is shown as three separate rays following from the entrance at the fiber slit through their diffraction at the grating to their incidence on the detector. The initial pink beam is the undiffracted light, while the diffracted light traces the path of different wavelengths (from blue to pink, 1975 Å $< \lambda <$ 2125 Å).

footprint, mounting the detector next to the fiber slit. A graphical overview of the optical design can be found in Figure 1. By placing the entrance slit image in the sphere at a distance equal to the radius of curvature of the grating, its diffracted image falls on a circle with that diameter, defined as a the Rowland circle (shown in Figure 2 by the dotted circle which comes into contact with the grating). More generally, the diffracted image of any object on the Rowland circle is known to lay close to the Rowland circle. In near Littrow conditions, the diffracted image is thus close to the object, and its image in the sphere is close to the entrance slit. This spectrograph has a very large annular FOV with good image quality.

The spectrograph is f/2.5 to match the numerical aperture of the input fibers, and the 1m telescope has a similar speed, to limit the loss due to focal ratio degradation (FRD) in fibers by using a spectrograph matched

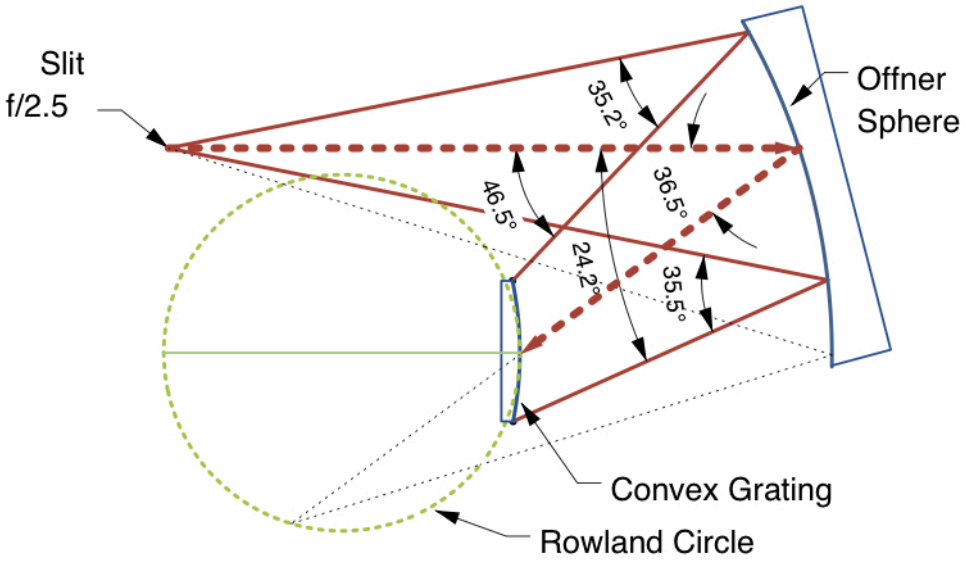

Figure 2. The spectrograph optical design. The Offner sphere, slit, and grating are marked. The imaginary rowland circle traced by the grating is also traced.

Table 2. Optical Requirements

Parameter	Value (+/-)
Mechanical Positioning	0.01 mm
Tilt	0.011 degrees
Defocus	50 μm

to the telescope. FRD is a common source of light loss in fiber applications, especially those which are installed on already built low speed systems.[1–3] FRD describes the cumulative effect of many different causes that change the output beam from fibers, including bending, core-cladding interface variations and overfilling the acceptance cone of the fiber or underfilling the input of the spectrograph. range of focal ratios from those fed to the fiber. FRD has been shown to be directly related to the input beam speed,[4] with faster systems losing a greater fraction of light to FRD. FRD is often a concern when fiber instruments are installed on ground based telescopes, which have had their design driven by different factors, often resulting in much slower beams where FRD leads to greater light loss. FIREBall has been able to avoid this particular problem by matching the input beam to the fiber's numerical aperture. The 1:1 (no magnification) design also provides a good match between the fiber size and the detector resolution.

Ultraviolet light is absorbed by common lens materials (fused silica, BK7). For materials which do transmit in the UV, such as single-crystal alkali halides, it can be prohibitively expensive to build large enough blanks with high enough quality for the lenses. By designing a system using only reflective optics (except for the fiber bundle) this materials issue is eliminated, as is the concern of chromatic aberrations inherent in transmissive optics. There was initial concern about the ability to achieve high reflectance in band, but the final coating for the large telescope and main spectrograph optic performed to specifications at $> 90\%$ reflectivity.

2.2 Mechanical Design and Alignment Requirements

The spectrograph is designed to be stable and secure for flight and landing, while providing maximum adjustability during the process of alignment. Table 2 shows the targted adjustable range for the mechanical design. As can be seen in Figure 3, the design is a two level hexapod mount. Carbon fiber legs provide stiffness while

being lightweight. The legs were mounted to the three optical mounting plates (top/detector, mid/grating, and bottom/sphere) using an angled mount block. This method reduces the overall system flexure by approximating the ideal hexapod (which has three mount points per plate, rather than six). Each hexapod leg is adjustable on both ends and differentially threaded to provide length adjustment by hand to 0.0036" (see section 6.2.1 for details on the hexapod).

The spectrograph was aligned by bringing the center of the Offner sphere into alignment with the center of the grating and then adding a small offset. The positioning precision required for the mounts is seen in table 2. These requirements fed the amount of adjustment built into the grating mount, as well as into the overall hexapod structure.

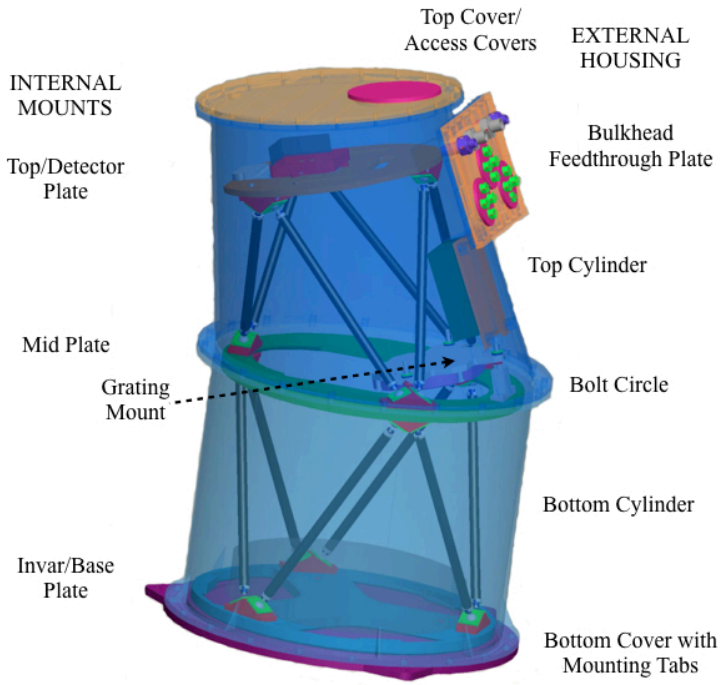

Figure 3. An overview of the spectrograph mechanical design. The inner hexapods are shown as black rods, but not labelled. A second access cover, not shown here, was added above the fibers to accommodate the vacuum feedthrough and ease adjustment of the fibers and detector.

We chose a simplified design in which we did not pursue in-flight focus, although the current flight mount includes a PI (Physik Instrumente) M110 stage that allows for that capability to be easily added with minor cabling and feedthrough changes. This low profile stage with reduced travel (15mm) was small enough to allow the top access cover to clamp shut, and performs repeatably against gravity while holding the fiber slit assembly. The stage was used to find best focus during spectrograph alignment.

The balloon platform is an exposed instrument environment, with large shifts in temperature and exposure to vibrations and shocks. We decided to enclose the entire spectrograph with a vacuum vessel, even though this weighs more than an uncovered design. The aluminum vacuum housing serves the multiple purposes of allowing the detector to operate at its optimal pressure throughout the flight, reducing temperature fluctuations within the spectrograph, baffling scattered light from throughout the gondola, and protecting the optics from mechanical interference and damage. Figure 3 shows the spectrograph enclosed in a rendering of the vacuum housing.

3. TECHNICAL CONSTRAINTS AND DESIGN CONSIDERATIONS

3.1 Bandpass Considerations

The NUV bandpass (1950 Å $< \lambda <$ 2300 Å) is limited by both atmospheric absorption and atmospheric emission. Absorption due to O_2 sets the short wavelength cutoff, while O_3 absorption sets the long wavelength cutoff. There are two nitric oxide (NO) sky bands (near 2100 Å) within the range where FIREBall currently observes. This emission varies with altitude and is not well measured or understood.[5] The overall throughput is also varying over the bandpass, as is shown in Figure 4, along with the three emission lines being targeted, with the appropriate redshift.

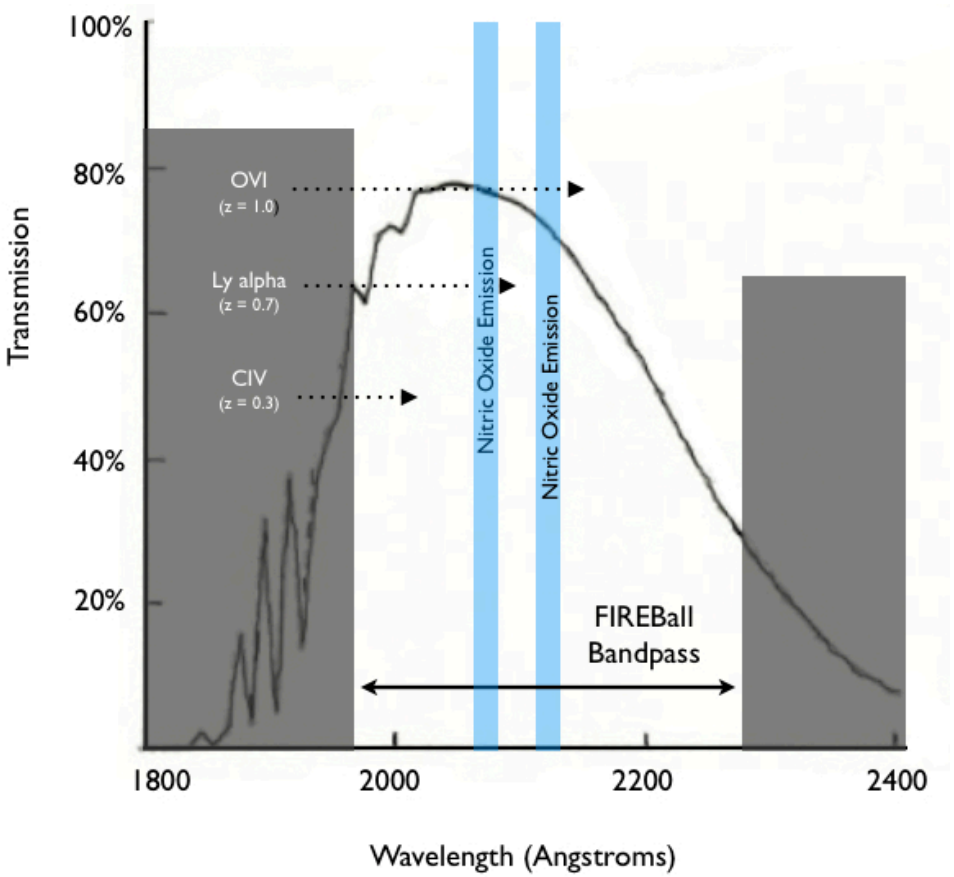

Figure 4. Atmospheric transmission at a pressure of 3 mbar.[6] The shape of the profile is caused by the overlapping O_2 and O_3 absorption profiles of the atmosphere. The wavelength range outside of FIREBall's bandpass (1900-2250 Å) has been grayed out but left visible to show the steep decline in transmission on both sides of the band. The two NO sky emission bands are shown in blue and labelled. For comparison, FIREBall's flight altitude for the second flight is the equivalent of $\sim$ 10 mbar. The emission lines FIREBall is searching for are shown with their redshifted positions in the band.

3.2 Detector Conditions

The atmospheric pressure at float altitudes of 30-40km are 1/100th to 1/1000th of an atmosphere. This "coronal" regime is dangerous for the high voltage microchannel plate detector used in the spectrograph. Field emission increases the frequency of dielectric breakdown and therefore arcing, causing sparks and shorts over the detector, rendering it inoperable.[7] We enclose the whole spectrograph and selected a flight pressure of 0.5 atmosphere. This provides enough atmospheric pressure for conduction of heat within the spectrograph while at the same time minimizing deflection of the housing which would increase with the pressure differential (constrained to less than 0.050").

Table 3. Spectrograph Mass Estimate

Component	Mass (kg)
Offner Sphere	23.0
Housing	75.1
High Voltage Power Supply (HVPS)	1.0
Detector and Amplifiers	2.0
Brackets/Mounts	3.0
Grating Hardware	3.62
Hexapod Legs	5.26
Mounting plates	58.5
TOTAL	171.48

3.3 Balloon Environment

Placing a scientific instrument on a balloon introduces unusual challenges. The platform is less stable, in many aspects, than any other available platform for observation. In particular, the range of temperatures and forces encountered is quite wide. The thermal survival range for the spectrograph and associated electronics was specified as -20° to 22° C, although as monitoring data reveals, the gondola experiences an even broader window during flight. The operating temperature was specified as $20° \pm 5°$ C. This is set by both the detector operating temperature, and the sensitivity of the gain to this parameter, as well as concerns of possible optical defocus with temperature variations. The balloon design also places some constraints on the spectrograph mass, placement, and footprint. Any available reduction in mass is valuable in that it increases the altitude (and access to our band) as can be seen in Figure 5.

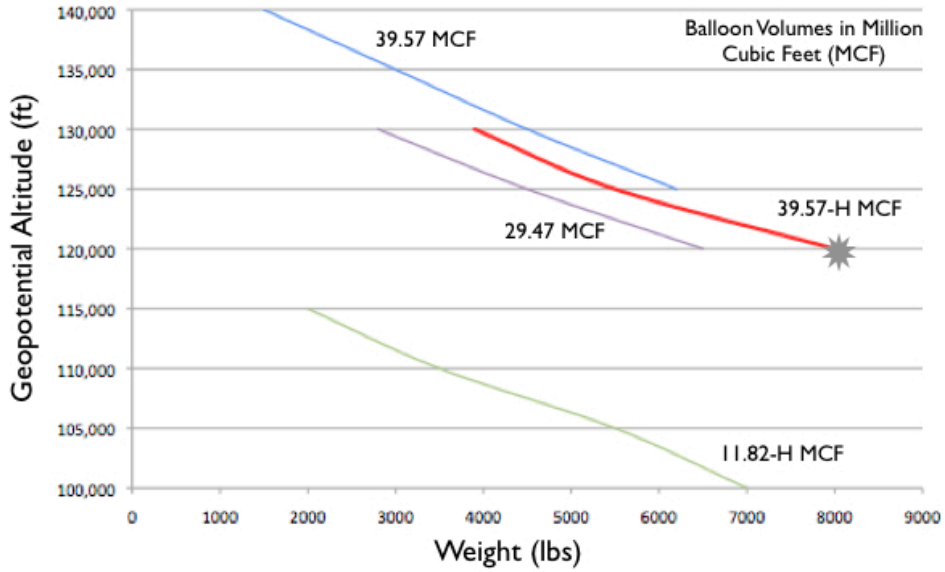

Figure 5. This plot shows the effect of payload mass on the altitude outcomes for various balloon volumes. For our second flight, FIREBall flew on a 39 Heavy MCF (Million Cubic Feet) volume balloon. The suspended weight versus altitude for this balloon can be found in the red line to the lower righthand side of the plot. FIREBall falls on the end of the 39H mass range, as shown by the grey star on the plot.

Table 4. Summary of Changes

Change	Motivation
Groove Density Change	Improve Reflectance
Black Interior of Spectrograph	Reduction of scattered light
Flight Ready Focus Stage	Improved testing conditions
	Option to focus slit during flight
Additional mount point for detector	Improved detector stability and positioning
Fiber Ferrule Redesign	Improved control of fiber bundle manufacture
	Improved kinematic mount in FPA
Increased bundle length	Reclaimed autocollimation mode
	Increased spectrograph placement flexibility
Slit end fiber redesign	Fixed curvature correction
	Spacing to improve spectral fitting

4. SUMMARY OF CHANGES BETWEEN FLIGHTS

Our experience during the first engineering flight resulted in a number of small changes to the spectrograph prior to the second flight. These changes are mentioned in the appropriate sections but are summarized in table 4. There are two main differences. First, the grating has been replaced with a slightly lower groove density version (R from 5000 g/mm to 4800 g/mm) which drives small changes in the assembly, alignment, and wavelength range. Secondly, the fiber bundle is of an improved design. The fiber length was better a fit for integration with the balloon, both the slit end and the focal plane end were redesigned with both data analysis and assembly conditions in mind after our experiences with the first flight. A flight ready stage was permanently incorporated into the fiber slit mount to improve our focus procedure. Small changes were made to the housing as well, with the inside of the cylinder body painted black to cut down on scattered light from the aluminum.

5. OPTICAL ELEMENTS

5.1 Fibers

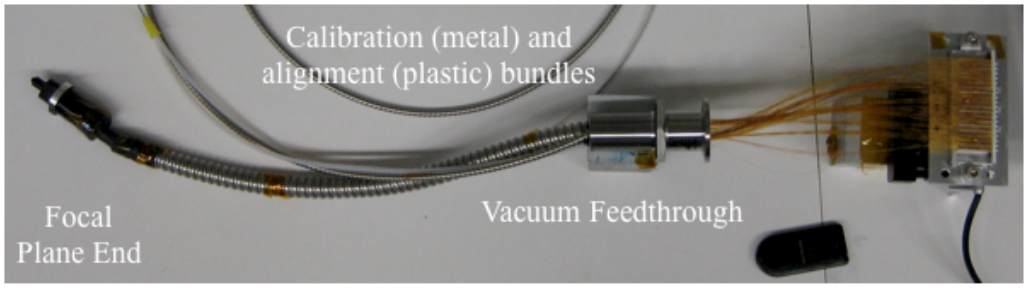

Figure 6. The flight 2 bundle. The calibration bundle and the alignment fibers come off the vacuum feedthrough to the top. The calibration bundle is wrapped in a smaller gauge stainless steel wrap like the science bundle. The alignment fibers (there are only 7) are in teflon tubing.

The second flight fiber bundle consisted of 281 science fibers connecting the focal plane to the spectrograph slit. The number was reduced from the first flight to increase our ability to identify individual spectra while maximizing our use of the detector area available. The focal plane bundle was a close packed hexagon unlike the circular random packing of the first flight, while the slit was packed edge to edge as in the first flight (Figure 6). The fiber assembly includes several auxiliary bundles, including seven focus fibers that had a reverse light path (from a lamp to the focal plane - used during auto-collimation), and a calibration bundle that connected a calibration box to fibers interspersed with the science fibers in the spectrograph slit. This scheme can be seen in Figure 7.

5.1.1 Fiber Slit

Figure 7. The two different slitlet designs used in Flight 2 are shownf here. The first design (A) was used on the outer teeth, giving more cleanly separated spectra in the final detector output. The central teeth had type B slits, giving more coverage. The filled fibers are scrap fibers, used for spacing. The red fibers are calibration fibers, with light piped from the calibration box.

Fibers are prepared individually, and then assembled into the spectrograph slit. The spectrograph slit was assembled in two stages. First, individual slitlets were assembled. A slitlet was one of two types (A or B), depending on the distribution of science, calibration, and buffer fibers. Individual fibers were polished as above. These fibers were then aligned into a slit and straightened, using a microscope for inspection. Epo-tek 302-3M epoxy was applied 2-3mm back from the fiber face. This prevented epoxy from wicking to the polished front surface, while constraining the three dimensional alignment of the fibers. After curing at room temperature, this slitlet was removed from the worktop and epoxied (again, under a microscope) to an aluminum tooth (7mm x 3mm front face). The polished fiber face protrudes slightly over the edge of the tooth to reduce the possibility of epoxy flow or reflections off the tooth front.

5.1.2 Focal Plane Bundle

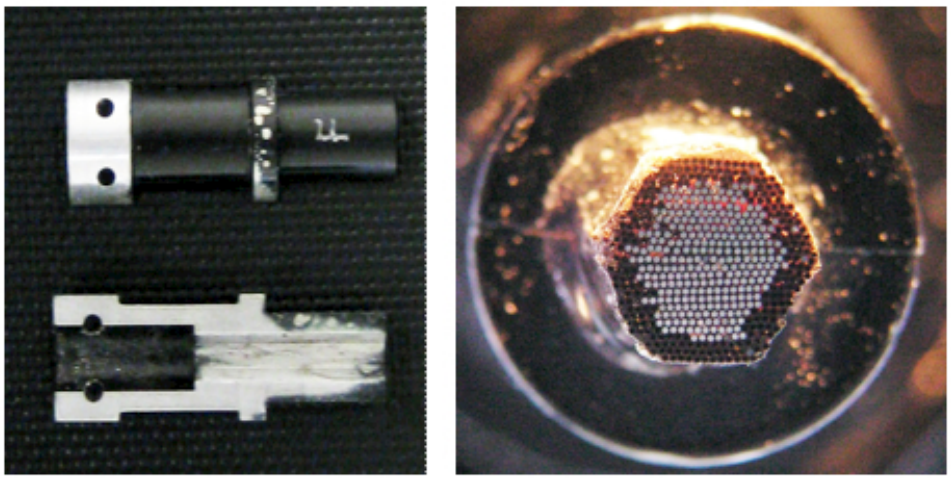

Figure 8. The focal plane fiber mold, shown with and without fibers. The two parts are machined together, along with an outer sheath, to ensure a snug fit. The letter "F" etched here identifies the set. The fibers are stacked row by row into the separate halves of the mold, then secured together to cure.

The focal plane end of the bundle consists of a close packed hexagonal bundle consisting of 281 science fibers and 7 focus fibers surrounded by three rounds of buffer fibers (Figure 8). The buffers protected the fibers both during polishing and during insertion into the focal plane. When polishing the large bundles, we found the edge row of fibers susceptible to curvature and occasionally to breakage. The bundle was assembled row by row, and then stacked into the two-part ferrule mold. The ordered and epoxied ends were left protruding from the mold so the cured epoxy didn't impede packing in the mold. These two pieces were injected with epoxy, sandwiched, and placed in the outer mold. The bundle was then cured for 24-48 hours before polishing. Fibers protruded two to three inches past the front face of the bundle. The bundle was cut to < 1" using a Dremel tool and then polished by hand down to the 2-3mm protrusion from the mold that allows alignment with the pinhole mask front surface.

Once the bundle is completed, the fibers (surrounded by the mold) are inserted into the outer ferrule. The two holes in the mold are aligned with the holes in the outer ferrule and are permanently attached via two pins.

Table 5. Optical Specifications And Coatings

	Offner Sphere	Grating (Flight 1)	Grating (Flight 2)
Diameter	480 mm	232mm	232mm
Radius of Curvature	880mm	470mm	470mm
Coating	Al + MgF_2	Al	Al + MgF_2
Coating Thickness	62nm + 41nm	proprietary	proprietary
Efficiency (at 200nm)	91%	20%	43%
Groove Density (g/mm)	n/a	5000	4800

5.1.3 Vacuum Feedthrough

A vacuum feedthrough was required to pass the fiber bundle through the spectrograph vacuum housing to feed the slit. The feedthrough was designed and built in house using an off the shelf o-ring bulkhead threaded feedthrough. A mask was machined to guide the fibers. The design both reduced the effective cross section and kept the fibers somewhat ordered. This was necessary since the fibers were mapped from the slit to the focal plane end of the bundle.

5.2 Offner Sphere

Two Offner blanks were manufactured by Winlight Optics in Marseille. The first sphere was coated by Tofico with bare aluminum. It had 82% efficiency at 200nm and was used for prototype construction and testing. The second sphere was coated by Goddard Space Flight Center. The coating is optimized for the waveband and is 62nm Aluminum overcoated with 41nm Magnesium Fluoride (MgF_2). Both coatings are deposited through evaporation. The MgF_2 overcoat protects against oxidization of the aluminum. It was measured to have a reflectance of 92% at 200nm. This coating also served as a test run for the large optics (primary and siderostat) used in the FIREBall telescope. The optical specifications for both the Offner sphere and the grating can be found in table 5.

5.3 Grating

The grating blank was figured by Winlight Optics. The convex grating was holographically ruled by Horiba Jobin-Yvon. The convex shape reduces the spherical aberration introduced by the Offner sphere. A laminar groove profile was used to enhance efficiency. The first grating had a measured efficiency which was half (20%) expected from theoretical values. This situation bears some resemblance to an occurrence during the manufacture of the COS gratings for HST. A combination of groove spacing and the MgF_2 overcoating appears to be causing a resonance efficiency anomaly.[8] A similar problem seems to have affected the FIREBall grating. This issue was resolved through replacement of the grating for the second flight. A thick MgF_2 and a decrease in the groove density to 4800 g/mm returned the efficiency to the theoretically predicted value of $\geq 40\%$.

5.4 Detector

The photon-counting detector used for both flights of FIREBall Gen-1 is a legacy GALEX NUV microchannel plate detector (MCP).[9] The z-stacked microchannel plate intensified detector operates at high voltage ($-5200V$) within a vacuum, sealed behind a concave plano fused silica window. The proximity focused Cesium Telluride (Cs2Te) photocathode is directly deposited on this window. The position is provided by cross delay line readout. The detector has a 65mm diameter visible area. This detector's low diffuse background of 1 count/cm/sec is a requirement for the faint objects we are observing. The detector does not require cooling. It operates optimally between 15° and 20° C (room temperature).

6. ASSEMBLY

6.1 Optical Bonding and Mounting

The reflective optics (the Offner sphere and the diffraction grating) were permanently mounted to machined plates with Dow RTV 3145 adhesive. The Offner sphere was mounted to an Invar (a nickel steel alloy) plate to reduce any chance of thermal distortion or other stress to the optic. The plate was light-weighted by removing large regions of the central mass, and leaving the rim and thick spoke-like supports which were stiff enough to support the optic. The Invar plate was then mounted to the spectrograph housing base plate. It is bolted at three equally spaced points around the diameter of the plate and decoupled using a thin plate between the Invar and the external housing.

The grating was mounted to an aluminum plate in the same method as the Offner sphere at the laboratory in Marseille. Since the grating is mounted inverted over the Offner sphere, small teflon safety catches were mounted at four points around the edges of the optic. They were left loose so no contact was made with the grating.

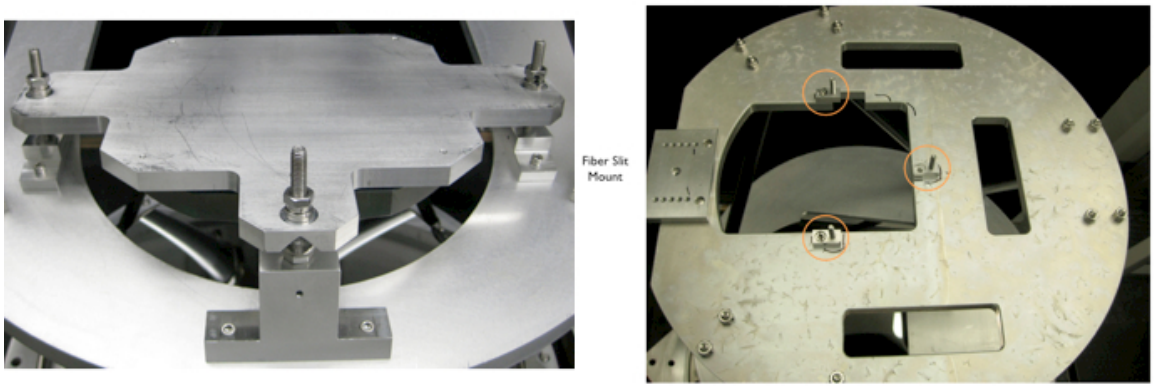

Figure 9. The left hand image shows the grating mount from the top down. Only a small portion of the back of the grating is visible. Spherical washers are mounted both top and bottom on the mounting rods. The ball washer on the bottom creates a kinematic mount in the groove on each mounting tab. The right image shows the top plate of the spectrograph, looking down into the instrument. The mounting plate for the fibers is also seen on the left here, with several threaded holes available to use as mount points for the fibers.

The grating is mounted by three rods angled off of the mid-plate as seen in Figure 9. The grating is secured using a locking ball nut on each side of the mount plate. The mount employs a spherical washer sitting within a groove joint, with the combination of the three making the mounting kinematic.

The detector is mounted face down on the top plate within the spectrograph. The detector has three tabs for mounting, one on each side, as seen in Figure 10. Figure 10 shows the top plate with the detector installed and cabled on the right hand side.

6.1.1 Fiber Slit Mounting

The fiber slit has two mounting tabs, one on each side of the tooth mount. These bolt to a plate which attaches, in the current flight 2 configuration, to the focus stage. The stage then mounts via two rods that are anchored to the top/detector plate. The position of these rods can be moved (several threaded holes are available in the plate) to adjust the distance between the slit and the detector. The assembly from two sides can be seen in Figure 11.

6.2 Internal Assembly

The spectrograph itself consists of a two layer hexapod frame shown in Figure 12. The right shows the three dimensional rendering, while the left shows the assembled frame. These legs allow for both adjustment of height and alignment of the optics. The Offner sphere is stationary. The grating has a three point mount secured with jam nuts. Both the fiber slit and the detector have a small amount of play, being fastened to the top plate using bolts. The sub systems are described below. The actual fiber slit mount is described in Section (6.1.1).

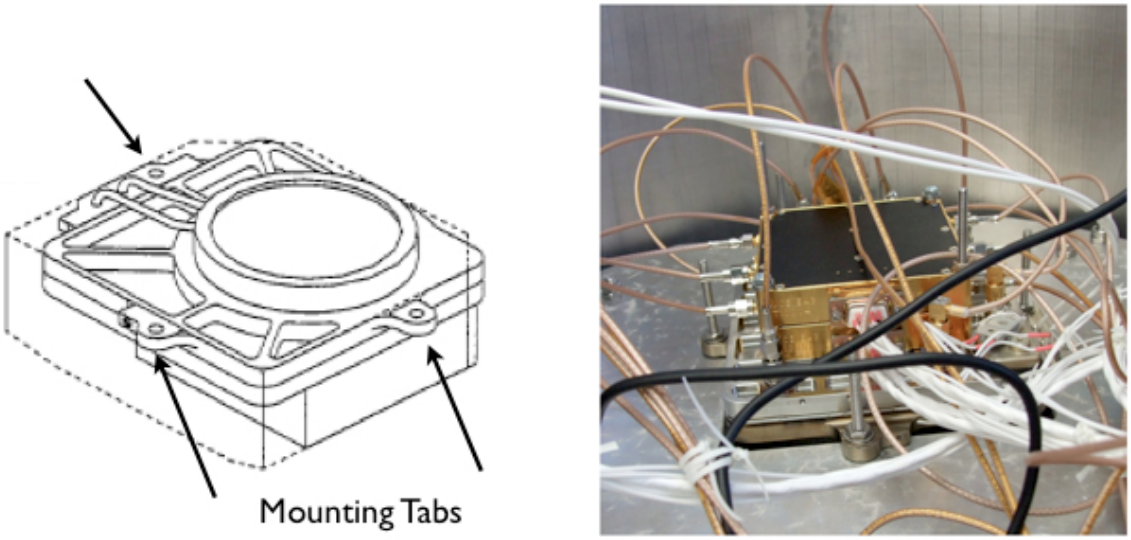

Figure 10. The machine drawing on the left shows both the mounting tabs on the detector, as well as the high voltage keep out zones for safety. The right image shows a photo of the top/back of the installed detector. The two gold stacked layers are the amplifiers.

6.2.1 Hexleg Design and Mounting

The hexleg design allows for two points of locking adjustment, one on each end of the carbon fiber leg. Inserted into each end is an assembly that ends in a smooth ball atop a threaded ball. Several views of this assembly can be seen in Figure 13. The assemblies were epoxied into the carbon fiber rods using AngströmBond 9119 and clamped for curing. All epoxy bonds have lasted through two flights and landings. Each assembly can be extended over several millimeters. The length was adjustable by twisting the carbon rod while holding one or both ball joints stationary. Each rod has one end with 1/4"-20 thread and the other end with a 1/4"-28 thread. If both ends are unlocked, this gives the ability to adjust the length 0.015" per turn. In our estimations we could easily discern 1/8 turns, giving the ability to control the length in steps of 0.0036. The hexlegs are mounted into an angled mount block on each plate of the spectrograph.

6.3 External Housing

The spectrograph is in a cylindrical aluminum vacuum housing. During flight, the housing is purged and backfilled with nitrogen to 0.5 atm. This allows us to maintain an ideal working environment for the detector within the spectrograph.

The external housing was constructed in two main cylindrical parts. This makes handling easier, and has also allowed us to implement an alignment mode. In alignment and testing mode, the top portion remains on while the lower portion is removed and replaced with steel H-bars wrapped in black out material.

6.4 Optical Scattering Reduction

The inside of the spectrograph housing was painted black using Aeroglaze before the second flight to decrease possible reflections and scattered light. At this point the remaining source of reflections is from the MCP detector. It should be masked before future flights if used again.

6.5 Thermal Control

Thermal control of the spectrograph is a combined active and passive system. The entire gondola is enclosed in a protective blanket. The blanket is white on the outside, and black on the inside, except for one side of the gondola where the white has been replaced with a reflective material. During the daylight hours, while the instrument is inoperable, the gondola is rotated so the reflective side faces the sun to minimize heating of the

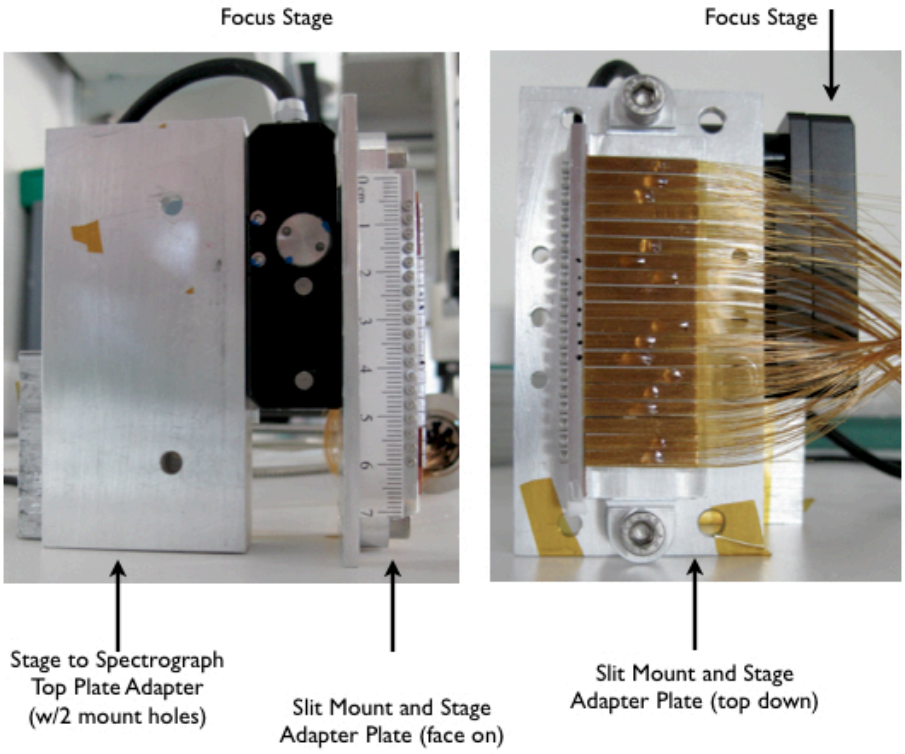

Figure 11. The fiber slit with associated mounting hardware. The left image shows the bundle face on. This face is mounted to face downwards in the spectrograph. The plate on the left with two holes is the mount interface with the detector plate in the spectrograph. The installed adapter plate has two threaded rods, and this whole fiber assembly is lowered into the spectrograph onto the mounting rods. The position is locked using nuts.

system. Keeping the system cool was important to limit the temperature change as the sun set, and to maximize use of available dark time.

The spectrograph had two patch heaters placed on the external housing, set to 23°C. These helped the spectrograph to maintain nominal operating temperature of 21°C. Thermal stability is important both to stabilize the detector gain and to hold the spectrograph focus.

7. OPTICAL ALIGNMENT

The optics are aligned mechanically first to meet the mechanical specifications. The hexleg lengths are set by hand during the build to the approximate length required for correct spacing between the three internal plates (top/detector, mid/grating, bottom/Invar). Once initial mechanical placement is correct, we use a faro arm to measure the mount plate and hexapod ball position precisely. The arm used provided accuracy to +/- 50 μm. The plate separations were adjusted until correct, and then the grating position was adjusted until the Offner sphere and the grating shared a common optical axis, although the true position is slightly offset in one direction.

After this alignment was achieved, the detector and fibers were installed for fine adjustment using the image. We combined a focus stage (PI M110) with the fiber mount for much of the fine alignment work. The shape of the spot was compared after focus runs with results of the Zemax model, to estimate the nature of the offset, and corrections were made both at the hexleg level and the grating level.

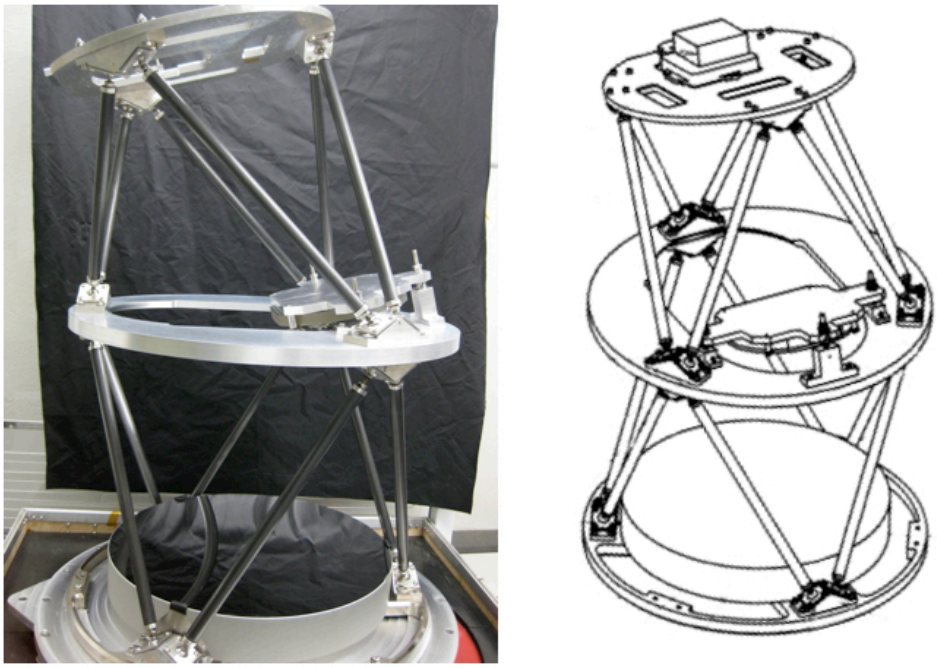

Figure 12. The internal structure of the spectrograph: On the right a rendering from the solidworks files, on the left an image after assembly. Both reflective optics are mounted.

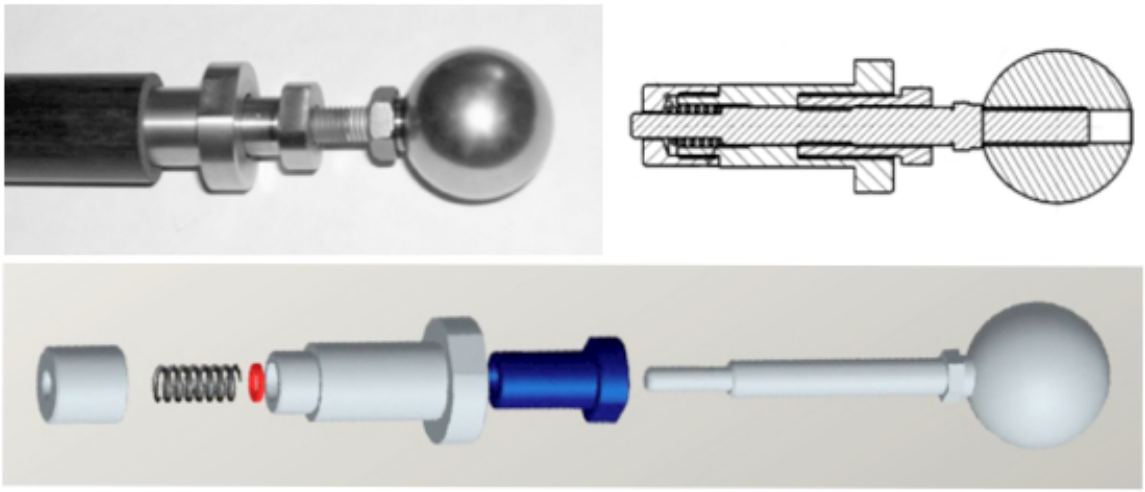

Figure 13. Here you see the ball end of each carbon fiber leg. The blue part highlighted in the bottom drawing is the locking collar. The aluminum piece closest to the carbon fiber is threaded, and is epoxied into the carbon fiber tube. When the carbon fiber tube is twisted, the assembly rotates around the threaded rod soldered into the ball.

8. INTEGRATION

8.1 Spectrograph Placement and Mounting

The bottom plate of the spectrograph housing has three tabs with bolt holes available for mounting. Two flex plates were designed to protect the spectrograph from flexure while mounting it securely to the gondola. The spectrograph is mounted directly to the gondola floor. The spectrograph was placed to minimize the length of the fiber bundle connection to the focal plane while avoiding interference with the frame or the siderostat.

8.2 Focal Plane

The fiber bundle is mounted into the focal plane block and clamped from the back (opposite the fiber face) into position. The cylindrical shape of the outer fiber mold, along with the machined flat perpendicular to the fiber face lock the fiber orientation against rotation. The optical surface of the fibers sits behind a dichroic that redirects the optical light into the guider camera for star tracking. An illumination bundle connected to the calibration box can also be inserted for ground-based calibrations in auto collimation mode.

8.3 Focus Performance

The spectrograph focus was set first during our initial integration at Caltech as a baseline in a controlled lab environment, and again once we had reached the field. The final stage of focus adjustment was correcting for the 1200mm curvature of the grating by adding curvature to the slit. This was done by placing teflon shims (.2mm) in between the fiber teeth and the fiber mount, and clamping them into position using the front screws. Three teeth on each side of the slit are shimmed, which adequately corrects for the focus degradation towards the edge of the slit.

Detector images are shown in Figure 14. The initial focus work was done with a test bundle using only calibration fibers so the number of spots is few (but it makes distinguishing the very out of focus spots easier). A near ideal spot was achieved for flight.

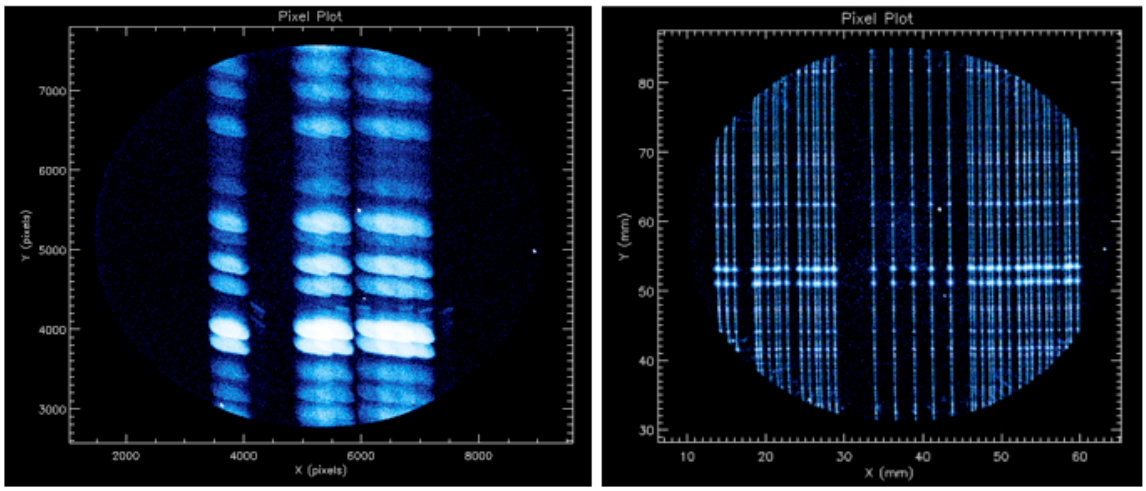

Figure 14. Focus after mechanical alignment (left) and after focus runs using the detector and focus stage (right). The first image uses a test bundle with a small number of fibers. The second image is the flight bundle calibration fibers illuminated with PtNe.

9. CONCLUSION

We have described above the FIREBall spectrograph design and assembly during the second flight. The spectrograph performed within specifications and is ready to be modified or flown again. Forthcoming publications will discuss the science results of initial measurements made with the spectrograph to constrain the emission of Lyman α, OVI and CIV from the IGM at $0.3 < z < 1.0$.

ACKNOWLEDGMENTS

The material is based upon work supported by NASA under award No. NNX08AO39G. The FIREBALL collaboration also acknowledges support from CNES, LAM and CNRS.

REFERENCES

[1] Ramsey, L. W., "Focal Ratio Degradation in Optical Fibers of Astronomical Interest," in [*Fiber Optics in Astronomy*], **3**, 26–40, Astronomical Society of the Pacific, San Francisco (1988).

[2] Wynne, C. G., "Telecentricity in fibre-fed spectrographs," *Monthly Notices of the Royal Astronomical Society* **260**, 307–316 (1993).

[3] Schmoll, J., Roth, M. M., and Laux, U., "Statistical Test of Optical Fibers for Use in PMAS, the Potsdam MultiAperture Spectrophotometer," *Publications of the Astronomical Society of the Pacific* **115**, 854–868 (July 2003).

[4] Carrasco, E. and Parry, I. R., "A method for determining the focal ratio degradation of optical fibres for astronomy," *Monthly Notices of the Royal Astronomical Society* **271**, 1–12 (1994).

[5] Laurent, J., Lemaitre, M.-P., Besson, J., Girard, A., Lippens, C., Muller, C., Vercheval, J., and Ackerman, M., "Middle atmospheric NO and NO2 observed by the Spacelab grille spectrometer," *Nature* **315**, 126–127 (1985).

[6] Donas, J., *No Title*, PhD thesis (1985).

[7] Scharfman, W. and Moritat, T., "Voltage Breakdown of Antennas at High Altitude," *Proceedings of the IRE* (November) (1960).

[8] Kuznetsov, I. G., Wilkinson, E., Content, D. A., Boucarut, R. A., and Madison, T. J., "Grating efficiencies comparison study: calculations versus metrology for various types of high groove density gratings at VUV-UV wavelengths," *Proceedings of SPIE* **5178**, 267–277 (2004).

[9] Siegmund, O. H. W., "The GALEX mission and detectors," *Proceedings of SPIE* **5488**, 13–24 (2004).